Biosci. Rep. (2012) / **32** / 35–44 (Printed in Great Britain) / doi 10.1042/BSR20100149

online data

Original Paper

Celecoxib reduces fluidity and decreases metastatic potential of colon cancer cell lines irrespective of COX-2 expression

Aslı SADE, Seda TUNÇAY, İsmail ÇIMEN, Feride SEVERCAN and Sreeparna BANERJEE[1]

Department of Biological Sciences, Middle East Technical University, Ankara 06531, Turkey

Synopsis

CLX (celecoxib), a selective COX-2 (cyclo-oxygenase-2) inhibitor, has numerous pleiotropic effects on the body that may be independent of its COX-2 inhibitory activity. The cancer chemopreventive ability of CLX, particularly in CRC (colorectal cancer), has been shown in epidemiological studies. Here we have, for the first time, examined the biophysical effects of CLX on the cellular membranes of COX-2 expressing (HT29) and COX-2 non-expressing (SW620) cell lines using ATR-FTIR (attenuated total reflectance–Fourier transform IR) spectroscopy and SL-ESR (spin label–ESR) spectroscopy. Our results show that CLX treatment decreased lipid fluidity in the cancer cell lines irrespective of COX-2 expression status. As metastatic cells have higher membrane fluidity, we examined the effect of CLX on the metastatic potential of these cells. The CLX treatment efficiently decreased the proliferation, anchorage-independent growth, ability to close a scratch wound and migration and invasion of the CRC cell lines through Matrigel. We propose that one of the ways by which CLX exerts its anti-tumorigenic effects is via alterations in cellular membrane fluidity which has a notable impact on the cells' metastatic potential.

Key words: attenuated total reflectance–Fourier transform IR (ATR-FTIR), celecoxib (CLX), colon cancer, cyclo-oxygenase-2 (COX-2), electron spin resonance (ESR), fluidity.

INTRODUCTION

CRC (colorectal cancer) is one of the leading causes of morbidity and mortality worldwide and chronic inflammation is accepted to have a significant effect in the promotion and progression of this disease [1]. COXs (cyclo-oxygenases) are key enzymes of the eicosanoid cascade that can convert arachidonic acid into prostaglandins, some of the important mediators of inflammation. The two COX isoforms, COX-1 and COX-2, have different expression patterns in the tissues, with COX-1 being constitutively expressed and with housekeeping functions such as gastrointestinal cytoprotection, renal functions and vascular homoeostasis. COX-2, on the other hand, is not expressed in most normal tissues and can be induced by a number of inflammatory stimuli, such as bacterial LPS (lipopolysaccharide), IL-1 (interleukin-1) and IL-2, and TNFα (tumour necrosis factor α) [2]. COX-2 is also overexpressed in the early adenoma stage of colon cancer [3]. It is not surprising therefore that NSAIDs (non-steroidal anti-inflammatory drugs) are associated with a reduced risk of colon cancer [4,5].

CLX (celecoxib) is a selective inhibitor of COX-2 which gives the advantage of reduced gastrointestinal bleeding compared with classical NSAIDs (e.g. acetylsalicylic acid and indomethacin) [6]. This new generation of NSAID has been indicated to relieve the symptoms of osteoarthritis and rheumatoid arthritis [6].

CLX has numerous pleiotropic effects in the human body, many of which are unrelated to its COX-2 inhibitory effects. According to epidemiological studies, long-term CLX usage is related to a chemopreventive activity in colorectal [7], breast [8] and lung carcinogenesis [9]. However, it is not clear whether CLX exerts its anticarcinogenic effects through a direct interaction with membrane-bound enzymes or whether its interaction with cellular membranes alters the activity of these enzymes. Amphipathic and lipophilic compounds, which can alter the biophysical characteristics of membrane lipids, are also able to alter membrane function by influencing the activity of integral membrane proteins [10–13]. CLX, being a lipophilic compound, is

Abbreviations used: ATR-FTIR, attenuated total reflection–Fourier transform IR; CLX, celecoxib; COX-2, cyclo-oxygenase-2; 16-DSA, 16-doxylstearic acid; DSPC, distearoyl phosphatidylcholine; EMEM, Eagle's minimum essential medium; IL, interleukin; MTT, 3-(4,5-dimethylthiazol-2-yl)-2,5-diphenyl-2*H*-tetrazolium bromide; NSAID, non-steroidal anti-inflammatory drug; RT–PCR, reverse transcription–PCR; SL-ESR, spin label–ESR; TNF, tumour necrosis factor.

[1] To whom correspondence should be addressed (email banerjee@metu.edu.tr).

also a potential modulator of membrane-lipid structure and dynamics which may account for its COX-2 independent activities [14].

Studies on membrane fluidity have been considered as a promising approach for cancer therapy since metastatic tumour cells have higher membrane fluidity compared with non-metastatic cells [15–17]. Using DSPC (distearoyl phosphatidylcholine) model membranes, we have previously shown that CLX decreases the fluidity of the membrane and induces phase separation of the lipids [18]. In the present study, we wanted to see if these effects of CLX were also valid in *in vitro* models and could account for the anticarcinogenic properties of CLX. We also wanted to determine whether COX-2 expression could affect these properties of CLX.

For that purpose, we have treated two different colon cancer cell lines, HT29 (COX-2 positive) and SW620 (COX-2 negative), with CLX, allowing us to delineate the COX-2-independent effects of CLX.

Using ATR-FTIR (attenuated total reflectance–Fourier transform IR) spectroscopy and SL-ESR (spin label–ESR) techniques, we investigated for the first time the alterations caused by CLX on lipid dynamics in the cell system. ATR-FTIR is used to study the structure, concentration and dynamics of macromolecules in biological systems [19–23]. Besides the ease of sample preparation, automated technology and the need for a small sample size, this technique allows rapid monitoring of functional groups in intact biological systems. In addition, the high sensitivity of the technique makes it a preferable tool for biodiagnostics and cell line discrimination [20,24,25]. ESR spectroscopy provides a sensitive way of determining lipid fluidity by the use of a spin probe that positions itself into the lipid bilayer [17,26]. Both these techniques have recently been applied to a breast cancer cell line for the characterization of microRNA-125b expression, by our group [22].

Following spectroscopic studies, we examined the effects of CLX on functional characteristics of colon cancer cells such as tumour cell proliferation, anchorage-independent growth, cellular migration and invasion. We propose that these changes may be independent of COX-2 expression status; rather, they may be associated with the changes in the membrane properties.

MATERIALS AND METHODS

Cell culture and reagents

The HT29 cell line was purchased from ŞAP Enstitüsü and grown in McCoy's 5a modified medium supplemented with 1.5 mM L-glutamine. The SW620 (CCL-227) cell line was purchased from the A.T.C.C. and grown in Leibovitz's L-15 medium supplemented with 2 mM L-glutamine. The normal colon fibroblast cell line, CCD-18Co (CRL1459), was purchased from the A.T.C.C. and propagated in EMEM (Eagle's minimum essential medium). The cells were grown in a humidified atmosphere containing 5 % CO_2 for HT29 and CCD-18Co and 100 % air for SW620. Cell culture media were supplemented with 10 % FBS (fetal bovine serum) and 1 % penicillin/streptomycin. All cell culture media and supplements were purchased from Biochrom.

CLX was obtained from Ranbaxy Laboratories and was dissolved overnight in molecular biology grade DMSO (Applichem) freshly before each treatment. The working concentration of DMSO in all treatments was adjusted to less than 0.1 %.

RNA isolation and RT–PCR (reverse transcription–PCR)

Total cellular RNA was extracted from HT29 and SW620 cells using the Rneasy Minikit (Qiagen) according to the manufacturer's instructions. First-strand cDNA synthesis was carried out from total RNA (1 μg) using oligo(dT)$_{18}$ primers and was PCR-amplified using COX-2-gene-specific primers (forward primer, 5′-TGCCTGGTCTGATGATGTATGCCA-3′; reverse primer, 5′-GCGGGAAGAACTTGCATTGATGGT-3′). After denaturing at 94°C for 3 min, the cDNA was subjected to 32 cycles of amplification at 94°C for 30 s, 60°C for 30 s and 72°C for 45 s, with a final extension at 70°C for 10 min. The PCR products were separated by gel electrophoresis on a 2 % agarose gel and visualized under UV transillumination.

Western blot analysis

Cell lysates were isolated using M-PER isolation buffer (Pierce) containing protease inhibitors (Roche). The protein content was measured using the modified Bradford assay using a Coomassie Plus protein assay reagent (Pierce). Whole-cell extracts (40 μg) were separated on a 10 % polyacrylamide gel and transferred on to a PVDF membrane (Bio-Rad Laboratories). The membrane was blocked in 5 % BSA and incubated overnight with COX-2 primary antibody (1:500 dilution; Santa Cruz Biotechnology) fol-lowed by incubation for 1 h with an HRP (horseradish peroxidase)-conjugated anti-rabbit (1:2000), secondary antibody. The bands were visualized using an enhanced chemiluminescence kit (ECL Plus; Pierce) according to the manufacturer's instructions.

ATR-FTIR spectroscopy

HT29 and SW620 cells were grown and treated with 20 μM CLX for 24 h in five separate flasks, and collected by trypsinization. Control cells (not treated with CLX) for both HT29 and SW620 were also grown and collected from five separate flasks. The cells were placed on the Di/ZnSe (diamond/ZnSe) crystal plate of the ATR-FTIR spectrometer (5 million cells/10 μl of PBS). The solvent was slowly evaporated under a gentle stream of N_2 flow for 30 min as described previously [22,23,27]. FTIR spectra were obtained using a Spectrum 100 FTIR spectrometer equipped with a Universal ATR accessory (PerkinElmer). Interferograms were averaged for 100 scans between 4000 and 650 cm^{-1} at 4 cm^{-1} resolution. The independent replicates for these experiments were carried out on different days to eliminate possible artefacts resulting from variations in ambient conditions. In order to ensure the same sample thickness, consistent sample

 ©The Authors Journal compilation ©2012 Biochemical Society

drying conditions and duration were maintained. Furthermore, each independent sample was scanned in three replicates under the same conditions by taking 10 μl from the same pellet of cells. The spectra were found to be identical for all the replicates. The results of the same sample were then averaged and used in detailed data and statistical analysis.

The spectra were analysed using Spectrum One software (PerkinElmer). The interfering spectrum of air was recorded together as background and subtracted automatically by the use of appropriate software. The band positions were measured according to the centre of weight and bandwidth was measured at 0.80×peak height position.

ESR spectroscopy

HT29 and SW620 cells were treated with a low dose (20 μM) and a high dose (40 μM for SW620 and 70 μM HT29) CLX in three separate flasks for 24 h and collected by trypsinization. Spin labelling of the cells was performed using the 16-DSA (16-doxyl-stearic acid) spin label as described previously [22,28,29]. Briefly, a stock solution of 16-DSA (10^{-2} M) was prepared by dissolving in ethanol, and was kept at -20°C. HT29 and SW620 cells were spin labelled by incubating a suspension of cells (5×10^{6} cells/ml PBS) for 60 min at 37°C to a final concentration of 10^{-4} M 16-DSA. Unbound spin labels were removed by washing the cells in PBS and centrifuging at 1200 ***g*** for 4 min until no free spin-label signal was observed in the supernatant.

For the ESR measurements, the cell film was transferred to a disposable glass capillary and ESR spectra were obtained at X-band, at 9.85 GHz, 100 G sweep width, 2 Gauss modulation amplitude and at 10 mW microwave power by using a Bruker EMX X-band (9–10 GHz). The membrane fluidity information was obtained from the calculation of the rotational correlation time (τ_c) as described previously [17,30].

Cellular proliferation

Cell proliferation was measured using the Vybrant MTT assay kit (Invitrogen) according to the manufacturer's guidelines. Briefly, 10 000 cells were plated in a final volume of 100 μl in complete McCoy, Leibovitz's medium or EMEM for HT29, SW620 and CCD-18Co cells respectively in 96-well tissue culture dishes. Cells were treated with CLX between the concentrations 20 and 100 μM in at least six replicates for each concentration. After 24, 48 and 72 h, the MTT [3-(4,5-dimethylthiazol-2-yl)-2,5-diphenyl-2*H*-tetrazolium bromide] labelling reagent was added, incubated for 4 h and solubilized with a 1% solution of SDS for another 4 h. The absorbance (A) was determined in a microplate reader (Bio-Rad Laboratories) at 570 nm.

In vitro scratch-wound healing assay

Cellular motility was measured by an *in vitro* scratch-wound healing assay. Equal number of SW620 or HT29 cells were seeded in six-well plates and incubated until they were 90% confluent. The monolayer of cells was scratched with a sterile pipette tip and debris was removed from the culture by washing twice with PBS. Images were captured immediately after wounding with an inverted microscope with ×4 objective (Olympus). The cells were then incubated in complete medium with or without CLX (40 μM for SW620 and 70 μM for HT29). Wound closure was monitored microscopically after the wound persisted for 72 h. The percentage wound closure between the wound edges were analysed using the ImageJ 1.42 program. The experiments were performed in three replicates.

Colony formation in soft agar

To evaluate the ability of cells to grow in an anchorage-independent manner, SW620 and HT29 cells (60000) were grown on Noble agar (Difco; BD Biosciences). The bottom agarose layer was prepared by layering 1 ml of complete medium with or without CLX (40 μM) containing 0.6% agar and allowing it to solidify for 1 h at room temperature (25°C) in a six-well plate. Cells were suspended in 400 μl of complete medium containing 0.33% agarose with or without 40 μM CLX. This solution (1 ml) was added on to the solidified bottom layer. After 2 weeks, the plates were stained with Crystal Violet (0.005%), the image was captured under a Leica light microscope with ×10 objective and the colonies were counted manually. Each experiment was performed in three replicates.

Boyden chamber cell migration and invasion assays

The effect of CLX on the migratory and invasive capabilities of HT29 and SW620 cells was determined by an *in vitro* Boyden chamber assay as described before [31]. The cell numbers used were: 5×10^{4} cells for both cell lines for the migration assay and 10×10^{4} cells for both cell lines for the invasion assay. Cells were treated with CLX (40 μM for SW620 and 70 μM for HT29) and allowed to migrate or invade for 72 h. The experiments were performed in six replicates for migration and five replicates for invasion assays.

Statistical analyses

Data analysis and graphing were carried out using the GraphPad Prism 5 software package. Unless otherwise mentioned, the mean for the indicated number of experiments was plotted together with the S.E.M. Statistical significance was assessed using two-tailed Student's t test. Significant difference was statistically considered at the level of $P \leqslant 0.05$.

RESULTS

Expression levels of COX-2 in HT29 and SW620 cells

The mRNA levels of COX-2 in HT29 and SW620 cells were determined by duplex semi-quantitative RT–PCR (Figure 1A). While HT29 expressed COX-2, no COX-2 mRNA expression was seen in SW620 cells. COX-2 protein levels were then determined

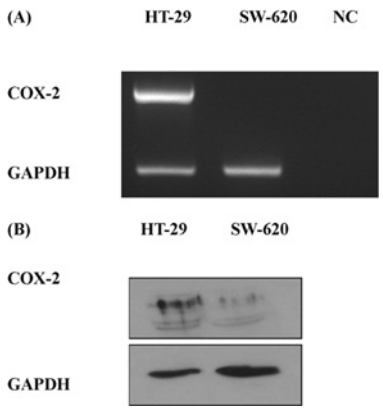

Figure 1 The HT29 cell line expresses COX-2 while the SW620 cell line does not
(A) mRNA and (B) protein levels of COX-2 in HT29 and SW620 cells were determined by RT–PCR and Western blot analysis respectively. GAPDH, glyceraldehyde-3-phosphate dehydrogenase.

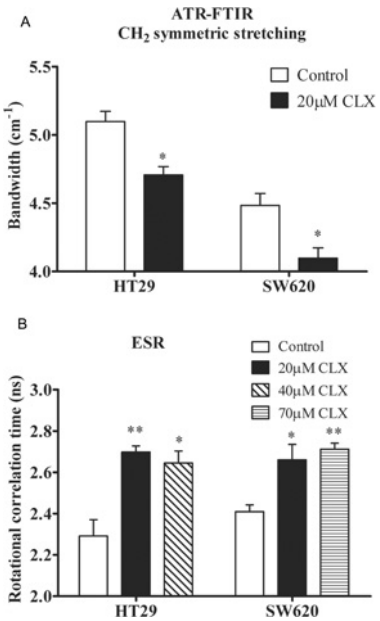

Figure 2 CLX reduces fluidity in the membranes of HT29 and SW620 cells
(A) ATR-FTIR: the average reduction in the bandwidth of the CH_2 symmetric stretching mode (indicating a reduction in fluidity) resulting from a 24 h treatment of HT29 and SW620 cells with 20 μM CLX are shown. (B) SL-ESR: the average increase in the rotational correlation time (indicating a reduction in fluidity) resulting from a 24 h treatment of HT29 and SW620 cells with a low (20 μM) and a high (70 μM for HT29 and 40 μM for SW620) dose CLX are shown. Each data point represents the means $\pm$ S.E.M. ($n = 5$ for FTIR and $n = 3$ for ESR). $*P < 0.05$ and $**P < 0.01$ compared with controls for each cell line.

by Western blot analysis (Figure 1B) and a negligible amount of protein was detected in SW620 cells, while HT-29 cells expressed a robust amount of COX-2.

CLX affects membrane fluidity in colon cancer cells

The effect of CLX treatment on membrane fluidity of HT29 and SW620 cells was determined by two non-invasive biophysical techniques, namely ATR-FTIR and SL-ESR.

In the ATR-FTIR study, five independently grown, CLX-treated and untreated sets of HT29 and SW620 cells were used. To obtain a homogenous film of cells, a mild N_2 stream was applied as reported by us and others in previous studies [22,23,27]. ATR-FTIR spectroscopy was used to monitor the changes in the cellular lipid dynamics by analysing the bandwidth of the spectral bands corresponding to lipids. The band position at 2850 cm^{-1} in a typical IR spectrum of a biological sample corresponds to the CH_2 symmetric stretching mode and results mainly from acyl chains of lipids. Information about the lipid dynamics can be obtained by analysing the variations in the bandwidth of the CH_2 stretching mode [22] and an increase in the bandwidth is an indication of an increase in the dynamics of the membrane system [32,33]. A representative IR spectrum of untreated and CLX-treated HT29 cells is shown in Supplementary Figure S1 (at http://www.bioscirep.org/bsr/032/bsr0320035add.htm) in which the difference in bandwidth of the CH_2 symmetric stretching mode can be seen in the inset. Similar spectra were also observed for SW620 cells (results not shown). Figure 2(A) shows the CLX-induced changes in the bandwidth of CH_2 symmetric-stretching band. For HT29 cells, the bandwidth decreased from 5.10 to 4.71 with CLX treatment ($*P < 0.05$), whereas for SW620 cells, a decrease from 4.48 to 4.10 was observed ($*P < 0.05$). This implies a reduction in lipid dynamics when the cells are treated with CLX.

The analysis of the frequency of CH_2 symmetric-stretching band to monitor acyl chain flexibility did not show a significant change. In addition, the changes in the frequency of the C=O stretching (1740 cm^{-1}) and PO_2^- antisymmetric double-stretching (1238 cm^{-1}) bands, which monitor hydration status of the glycerol backbone and lipid head groups respectively, were not significant (Supplementary Figure S2 at http://www.bioscirep.org/bsr/032/bsr0320035add.htm).

The reduction in lipid dynamics was also confirmed by ESR spectroscopy. 16-DSA is a stearic acid analogue, having a nitroxide radical ring at the 16th carbon position of its acyl chain. The molecule positions itself along the acyl chain of the lipid bilayer that monitors the hydrophobic interior of the membrane [28]. The signal coming from the nitroxide radical is directly affected by the biophysical characteristics of its immediate environment and the rotational correlation time (τ_c) calculated from the ESR spectrum is inversely correlated with the fluidity of the membrane [22,26,34]. A representative ESR spectrum of untreated and CLX-treated cells is given in Supplementary Figure S3 (at http://www.bioscirep.org/bsr/032/bsr0320035add.htm). Figure 2(B) shows the CLX-induced changes in the fluidity of the cell membrane reflected by the rotational correlation time. A low (20 μM) and a high (40 μM for SW620 and 70 μM HT29) concentration of CLX were used for each cell line in order to see the effect of different doses of the drug. As seen in the Figure,

©The Authors Journal compilation ©2012 Biochemical Society

Table 1 IC_{50} values for the inhibition of cellular proliferation in HT29, SW620 and CCD-18Co cells after 24, 48 and 72 h treatment with CLX (0–100 μM)

		IC_{50} value		
CLX treatment time (h)	**Cell line . . .**	**HT29**	**SW620**	**CCD-18Co**
24		122 ± 5.3	56 ± 2.2	119 ± 5.3
48		70 ± 3.9	47 ± 3.0	73 ± 4.7
72		41 ± 2.9	49 ± 3.4	67 ± 4.1
Mean		78	51	86

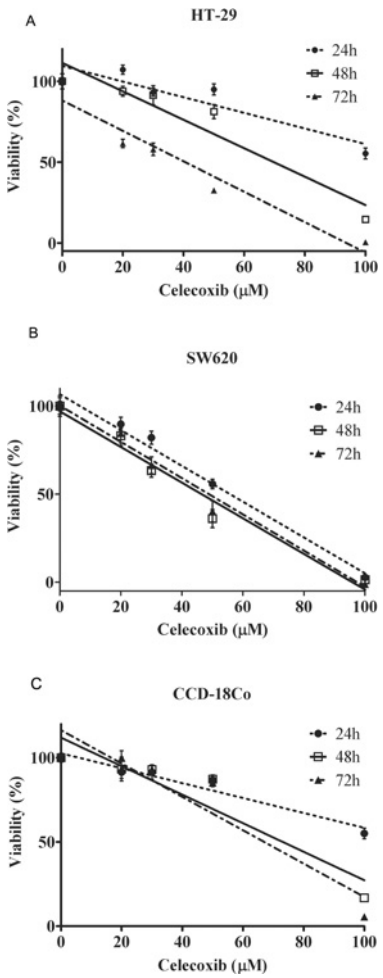

Figure 3 The effect of CLX on the proliferation of HT29, SW620 and CCD-18Co cells

HT29 (A), SW620 (B) and CCD-18Co (C) cells were placed in 96-well plates and treated with 20, 30, 50 and 100 μM CLX for 24, 48 and 72 h. The cellular proliferation was determined for each time point by an MTT assay. Each point represents the means ± S.E.M. ($n = 10$ for SW620 and HT29 and $n = 6$ for CCD-18Co).

the rotational correlation time increases significantly with CLX treatment for both cell lines indicating a decrease in membrane fluidity, which is consistent with our FTIR results. An approximate increase of 15 % in the τ_c is observed for both low and high concentrations of the drug.

Effects of CLX on cellular proliferation, motility and anchorage-independent growth

The sensitivity of HT29 and SW620 cell proliferation to CLX was determined by the colorimetric MTT cell proliferation assay. CCD-18Co, a non-transformed colon fibroblast cell line, was also included in order to compare the effect of the drug in cancerous and normal cells. CLX induced a decrease in proliferation in all cell lines in a dose-dependent manner (Figures 3A–3C). However, for both HT29 and CCD-18Co non-transformed fibroblast cell lines, but not SW620, a time-dependent decrease in proliferation was also observed (Table 1). Surprisingly, the effective dose needed to reduce the proliferation by 50 % (IC_{50}) for the COX-2 positive HT29 cell line (average IC_{50} values for 3 days: 78 μM; Figure 3A) was found to be higher than that of COX-2 negative SW620 (average IC_{50} values for 3 days: 51 μM; Figure 3b). This implies that the antiproliferative effect of CLX could be independent of the COX-2 expression status. In addition, the IC_{50} for the normal colon cell line, CRL1459, was found to be the highest (average IC_{50} values for 3 days: 86 μM; Figure 3c). The DMSO concentration (0.1 %) used in the present study showed no significant effect on cell viability (results not shown). The IC_{50} values determined in the MTT assay were taken as the maximum CLX concentration to be used in the consequent experiments in order not to confuse inhibition of proliferation with inhibitory effects on other functional characteristics such as cellular motility, migration and invasion.

In order to determine the effect of CLX on the motility of HT29 and SW620 cells, an *in vitro* scratch-wound healing assay was performed. Figure 4(A) displays the pictures of the wound at the day of application and after 72 h of incubation for HT29 and SW620 cells. As seen in the histogram in Figure 4(B), CLX treatment (70 μM for HT29 and 40 μM for SW620) significantly reduced percentage wound closure; indicating a loss in the motility of HT29 ($^*P < 0.05$) and SW620 ($^{**}P < 0.01$) cells after 72 h.

The influence of CLX on the anchorage-independent growth capacity of HT29 and SW620 cells was investigated using the soft agar assay for colony formation. The results shown in Figure 5 indicate that CLX treatment (40 μM) significantly decreased the number of colonies formed by HT29 ($^*P < 0.05$) and SW620 ($^{**}P < 0.01$) cells. In addition, the size of the colonies formed by

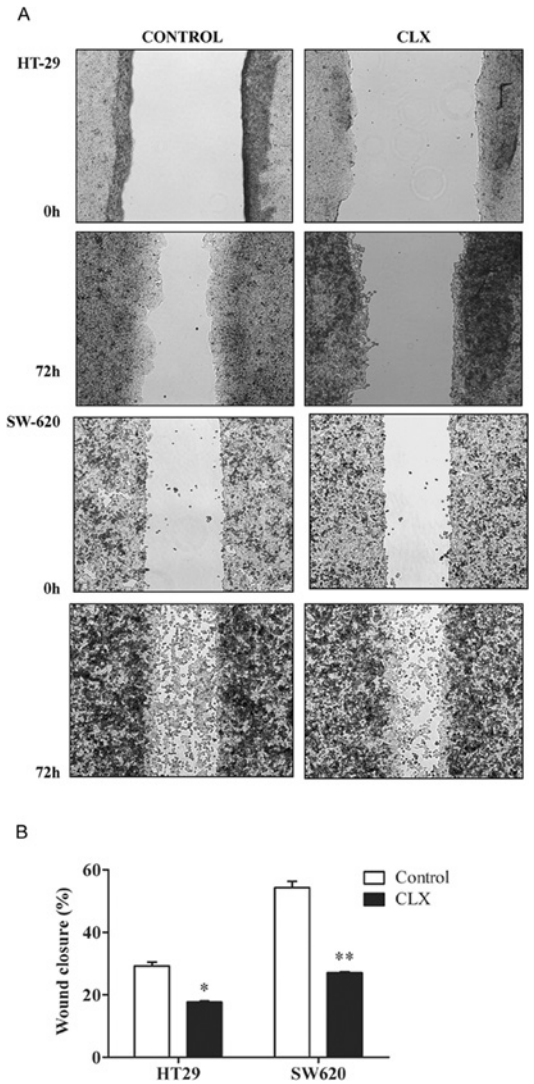

Figure 4 CLX reduces cellular motility of HT29 and SW620 cell lines

(A) A scratch-wound healing assay was conducted and inverted microscope images (×4) for 72 h CLX treatment (70 μM for HT29 and 40 μM for SW620) are given. Cells treated with CLX were not able to close the wound in the confluent culture, when compared with untreated control cells, after 72 h. (B) The histogram shows that CLX-treated cells significantly reduced motility ($*P < 0.05$) in HT29 cells with 18% wound closure for treated cells compared with 29% for untreated cells. The same was for SW620, 27% for CLX-treated cells and 54% for untreated cells ($**P < 0.01$). The results are the means ± S.E.M. for three independent experiments for both cell lines.

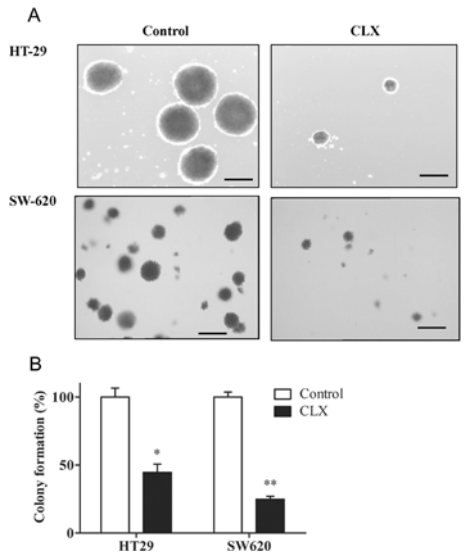

Figure 5 CLX treatment decreases anchorage-independent growth on soft agar

(A) HT29 and SW620 cells were treated with 40 μM CLX and grown on 0.6% Noble agar for 2 weeks. Colonies were stained with 0.005% Crystal Violet and counted under a light microscope. (B) The histogram shows that cells treated with CLX formed significantly fewer colonies (45% for HT29, $*P < 0.05$ and 25% for SW620, $**P < 0.01$) compared with untreated cells (colony formation represented as 100%). Error bars represent three independent experiments carried out in triplicate. The scale bars for all figures indicate 100 μm.

both cell lines was smaller in the CLX-treated samples compared with control ones.

Effects of CLX on the migratory and invasive characteristics of colon cancer cells

In order to assess how CLX alters the migration and invasion of HT29 and SW620 cells, *in vitro* cell migration and Matrigel invasion assays were performed based on the principle of the Boyden chamber assay. The migration assay was carried out by adding the cells in medium to Transwell inserts containing membranes with 8-μm-diameter pores. Figure 6 shows the representative pictures and results for the CLX-treated HT29 (70 μM CLX) and SW620 (40 μM CLX) cells. The results indicate that CLX caused a significant decrease in the number of migrated cells for both HT29 ($**P < 0.01$) and SW620 ($***P < 0.001$) cells.

The invasion assay was carried out by adding the cells in medium to Transwell inserts containing membranes with 8- μm-diameter pores coated with Matrigel which served as a reconstituted basement membrane *in vitro*. CLX treatment significantly ($**P < 0.01$ for both cell lines) decreased the invasive capacity of both colon cancer cell lines (Figure 7).

DISCUSSION

In the present study, the effects of CLX on the biophysical properties of the cellular lipids of two colon cancer cell lines, HT29 (COX-2 positive) and SW620 (COX-2 negative), and functional characteristics of the cell lines upon treatment with the drug were investigated. We have observed that CLX-inhibited cellular proliferation significantly in both cell lines irrespective of the COX-2

©The Authors Journal compilation ©2012 Biochemical Society

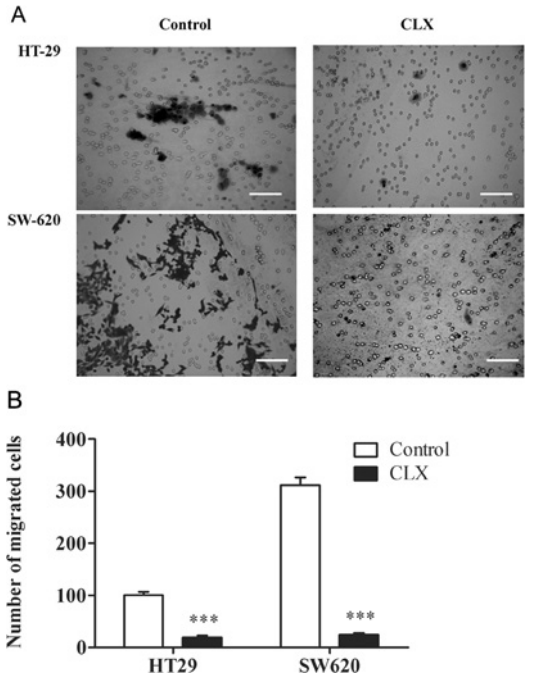

Figure 6 CLX treatment reduces cellular migration of HT29 and SW620 cell lines

(A) A Transwell migration assay was performed in the presence of serum as a chemoattractant. (B) The histogram shows that CLX-treated HT29 and SW620 cells migrated through the 8 μm pores of the Transwell in significantly less numbers (***$P < 0.001$) compared with the untreated control cells. The representative images ($\times$4) for CLX treatment (70 μM for HT29 and 40 μM for SW620) for 72 h are given. The histogram shows the means $\pm$ S.E.M. for six independent experiments for both cell lines. The scale bars for all panels indicate 40 μm.

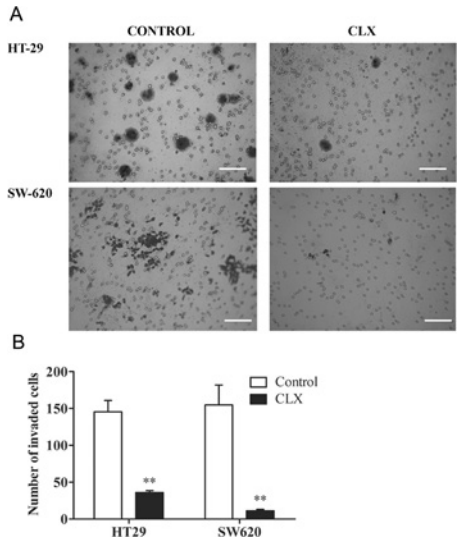

Figure 7 CLX reduces the invasive characteristics of HT29 and SW620 cell lines

(A) A Transwell invasion assay was conducted to determine the ability of CLX-treated HT29 and SW620 cells to invade through Matrigel, a reconstituted basement membrane. CLX-treated HT29 and SW620 cells invaded through Matrigel in significantly less numbers (**$P < 0.01$) compared with the untreated control cells. The representative images ($\times$4) for CLX treatment (70 μM for HT29 and 40 μM for SW620) for 72 h are given. (B) The histogram shows the means $\pm$ S.E.M. for five independent experiments for both cell lines. The scale bars for all of the panels indicate 40 μm.

expression status. Additionally, CLX also inhibited the proliferation of a non-transformed colon fibroblast cell line CCD-18Co, although the IC_{50} value (86 μM) for inhibition was higher than that for the cancer cell lines HT29 (78 μM) and SW620 (51 μM). The fact that the inhibitory dose needed for SW620 cells was less than that of HT29 cells indicates a possible involvement of mechanisms other than COX-2 inhibition.

It has been reported that the anticarcinogenic effects of CLX can be observed only at higher doses (800 mg/day) than that which is recommended for its anti-inflammatory efficacy (200 mg/day) [35,36]. In addition, owing to the high hydrophobicity of the drug, the maximum plasma concentration achieved after the administration of 800 mg/day CLX is 3–5 μM, which is far lower than the concentrations used in this and previous *in vitro* studies [35]. However, Maier et al. [37] have recently shown that CLX accumulates in the hydrophobic interior of the plasma membranes of different tumour cell types and proposed that a high intracellular drug concentration may explain the anticarcinogenic effects. Therefore the CLX concentrations used in the present study (20–70 μM), although higher than the amount found physiologically in the plasma, was required to observe the effects reported, and supports the necessity for higher intracellular drug concentration for its antitumorigenic efficacy.

FTIR spectroscopy is based on monitoring the energy absorbed between vibrational energy levels of different functional groups belonging to macromolecules. Therefore it gives a spectrum unique to the system where the bands assigned to different functional groups can be monitored simultaneously. In the past decade, this technique has been successfully applied to the identification of malignancies [21] and drug resistance in cell lines [27] as well as to discriminate between cancerous and normal tissues for diagnostic purposes in breast, colon, cervical and prostate cancers [20,24,25,38]. Furthermore, this technique has successfully been applied to monitor lipid fluidity in cells and tissues [22,39]. Here, using an *in vitro* system of colon cancer cell lines, we have shown a decrease in the bandwidth of the CH_2 symmetric stretching band indicating that 20 μM CLX decreases the lipid fluidity of both cell lines. This finding was also supported by ESR spectroscopy, which is a widely accepted technique for studying membrane fluidity [22,26,29,34]. In addition, we have found that there is no significant difference between the effect of low and high concentrations of CLX on membrane fluidity for both cell lines. This indicates that the fluidity of the membranes of HT29 and SW620 cells are similar regardless of the concentration of CLX used in the present study. Similar effect of CLX on reducing membrane fluidity was also reported by us on DSPC model membranes [18] as well as by Gamerdinger et al. [14], where a mouse neuroblastoma cell line

N2a was used. In addition, the magnitude of the change in the spectral parameter reflecting fluidity in our study (10–15%) is also similar to that reported by Gamerdinger et al. [14] (10%) in which steady-state fluorescence anisotropy was used. Interestingly, no significant change in lipid order (acyl-chain flexibility) and strength of H-bonding around the phosphate head-group and glycerol backbone was observed. This clearly indicates that CLX exerts its effect by specifically changing the fluidity of the lipids.

Lipid order and fluidity are important parameters for the proper functioning of biological membranes which, in turn, influence cellular processes and disease states [10,13]. For instance, membranes of cancerous cells have been found to possess higher fluidity compared with membranes of non-tumour cells [40]. An anticancer drug, tamoxifen, was also found to reduce membrane fluidity that was proposed to be an additional mechanism for its anti-tumorigenic action [33,41]. Other NSAIDs such as aspirin and etoricoxib, which are known to have chemopreventive potential, were found to restore the increased fluidity of colonic brush-border membranes in a 1,2-dimethylhydrazine-induced colon carcinogenesis model in rats [42]. In addition, several studies on cancer metastasis have revealed that increased membrane fluidity is associated with metastatic properties such as motility and invasion [15,16,43], which could thus be counteracted by the ability of CLX to decrease membrane fluidity.

In the present study, we therefore examined whether the decreased fluidity observed by biophysical studies was reflected in the actual abrogation in the metastatic potential of the cancer cell lines upon treatment with CLX. We have observed that CLX could reduce cellular motility regardless of COX-2 expression in both HT-29 and SW620 cells as assessed by the scratch-wound healing assay.

Anchorage-independent growth is accepted as an *in vitro* characteristic of neoplastic cells [31]. Our results indicate that treatment with CLX reduces the number and size of colonies formed by HT29 and SW620 cells on soft agar and thereby inhibits the ability of these cells to grow in an anchorage-independent manner.

Next, we examined the migratory and invasive characteristics of HT29 and SW620 cells through Transwell insert membranes. CLX significantly reduced the ability of both cell lines to migrate through the Transwells. Invasion was assessed using Matrigel as an *in vitro* reconstituted basement membrane and both cell lines lost their capacity to invade the basement membrane when treated with CLX. Considering the fact that both cell lines were affected similarly in all of the assays regardless of COX-2 expression, we can conclude that CLX may exert its anti-tumorigenic effects independently of COX-2 inhibition. These findings are also consistent with other studies stating that the antitumorigenic properties, rather than COX-2 inhibitory activity, gain precedence at high doses (50 μM) [35,44].

Metastasis involves the interaction of adhesion molecules and their ligands in order for the tumour cells to intravasate through the vascular endothelium into distant metastasis sites [45]. More fluid domains enhance lateral diffusion of ligands involved in binding to adhesion molecules. Additionally, some death receptors have been found to organize into microdomains or lipid rafts which enhances cell apoptosis [17,46]. CLX has also been proposed to form domains by us and others [18,47] and shown to enhance co-localization of specific proteins such as APP (amyloid precursor protein) and its cleaving enzyme BACE1 (β-site amyloid precursor protein-cleaving enzyme 1) within DRMs (detergent resistant membranes) [14]. Therefore a possible mechanism for the loss in metastatic potential of the cells upon CLX treatment may stem largely from the ability of the drug to reduce the fluidity in the cell membranes.

CLX has been shown to act independently of COX-2, through other signalling molecules or enzymes such as the inhibition of PDK1 (phosphoinositide-dependent kinase 1) in prostate cancer cells [48], increasing the levels of ceramide in mammary tumour cells [49] or through transcription factor NF-κB (nuclear factor κB) [50] (for a review, please see [5]). However, it is not clear whether these enzymes are direct targets of CLX or whether the drug exerts its action through indirect mechanisms. Several lines of evidence have shown that the modifications of physical characteristics of membrane bilayers leads to altered membrane enzyme activities, permeability of ion channels and membrane-bound receptors [40,51]. In a recent study, where cholesterol-like effects of CLX on cellular membranes were investigated, CLX has been shown to inhibit the activity of SERCA (sarcoplasmic/endoplasmic reticulum Ca^{2+}-ATPase) and it has been proposed that this inhibition is very closely correlated with the decrease in membrane fluidity [14].

As a conclusion, we investigated the effects of CLX on structural and dynamic properties of cellular membranes of colon cancer cell lines, HT29 and SW620. CLX was found to decrease the fluidity of the cellular membranes and inhibit proliferation, migration and invasion of both colon cancer cell lines, regardless of COX-2 expression. While it is likely that the anticarcinogenic properties of CLX may result from direct targeting of signalling pathways, we propose that changes in biophysical characteristics of membranes such as the decrease in membrane fluidity caused by the drug may also account for these effects. The association between the changes in the membrane properties and anticarcinogenic effects of CLX should further be elucidated.

AUTHOR CONTRIBUTION

Asli Sade carried out the ATR-FTIR and ESR experiments, and wrote the manuscript; Seda Tunçay and Ismail Çimen carried out the cancer cell functional assays; Feride Severcan supervised the FTIR and ESR research; and Sreeparna Banerjee oversaw the research, provided guidance and wrote the paper.

ACKNOWLEDGEMENTS

We thank the Turkish Atomic Energy Authority for allowing us to use their ESR facility, and Dr Muharrem Büyüm and Nihal Şimşek Özek for their assistance during the ESR studies.

 ©The Authors Journal compilation ©2012 Biochemical Society

FUNDING

This study was supported by the Scientific Research Funds of Middle East Technical University [grant number BAP- 07-02-2010-05 (to S.B.)].

REFERENCES

1 Danese, S. and Mantovani, A. (2010) Inflammatory bowel disease and intestinal cancer: a paradigm of the Yin-Yang interplay between inflammation and cancer. Oncogene 29, 3313–3323
2 Funk, C. D. (2001) Prostaglandins and leukotrienes: advances in eicosanoid biology. Science 294, 1871–1875
3 Shiff, S. J. and Rigas, B. (1999) The role of cyclooxygenase inhibition in the antineoplastic effects of nonsteroidal anti-inflammatory drugs (NSAIDs). J. Exp. Med. 190, 445–450
4 Stoner, G. D., Budd, G. T., Ganapathi, R., DeYoung, B., Kresty, L. A., Nitert, M., Fryer, B., Church, J. M., Provencher, K., Pamukcu, R et al. (1999) Sulindac sulfone induced regression of rectal polyps in patients with familial adenomatous polyposis. Adv. Exp. Med. Biol. 470, 45–53
5 Grosch, S., Maier, T. J., Schiffmann, S. and Geisslinger, G. (2006) Cyclooxygenase-2 (COX-2)-independent anticarcinogenic effects of selective COX-2 inhibitors. J. Natl. Cancer Inst. 98, 736–747
6 Goldenberg, M. M. (1999) Celecoxib, a selective cyclooxygenase-2 inhibitor for the treatment of rheumatoid arthritis and osteoarthritis. Clin. Ther. 21, 1497–1513
7 Bertagnolli, M. M., Eagle, C. J., Zauber, A. G., Redston, M., Solomon, S. D., Kim, K. M., Tang, J., Rosenstein, R. B., Wittes, J., Corle, D. et al. (2006) Celecoxib for the prevention of sporadic colorectal adenomas. N. Engl. J. Med. 355, 873–884
8 Harris, R. E., Beebe-Donk, J. and Alshafie, G. A. (2006) Reduction in the risk of human breast cancer by selective cyclooxygenase-2 (COX-2) inhibitors. BMC Cancer. 6, 27
9 Harris, R. E., Beebe-Donk, J. and Alshafie, G. A. (2007) Reduced risk of human lung cancer by selective cyclooxygenase 2 (COX-2) blockade: results of a case control study. Int. J. Biol. Sci. 3, 328–334
10 Korkmaz, F., Kirbiyik, H. and Severcan, F. (2005) Concentration dependent different action of progesterone on the order, dynamics and hydration states of the head group of dipalmitoyl-phosphatidylcholine membrane. Spectrosc. Int. J. 19, 213–219
11 Lucio, M., Ferreira, H., Lima, J., Matos, C., de Castro, B. and Reis, S. (2004) Influence of some anti-inflammatory drugs in membrane fluidity studied by fluorescence anisotropy measurements. Phys. Chem. Chem. Phys. 6, 1493–1498
12 Knazek, R. A., Liu, S. C., Dave, J. R., Christy, R. J. and Keller, J. A. (1981) Indomethacin causes a simultaneous decrease of both prolactin binding and fluidity of mouse-liver membranes. Prostaglandins Med. 6, 403–411
13 Maxfield, F. R. and Tabas, I. (2005) Role of cholesterol and lipid organization in disease. Nature 438, 612–621
14 Gamerdinger, M., Clement, A. B. and Behl, C. (2007) Cholesterol-like effects of selective cyclooxygenase inhibitors and fibrates on cellular membranes and amyloid-β production. Mol. Pharmacol. 72, 141–151
15 Nakazawa, I. and Iwaizumi, M. (1989) A role of the cancer cell-membrane fluidity in the cancer metastases: an ESR study. Tohoku J. Exp. Med. 157, 193–198
16 Taraboletti, G., Perin, L., Bottazzi, B., Mantovani, A., Giavazzi, R. and Salmona, M. (1989) Membrane fluidity affects tumor-cell motility, invasion and lung-colonizing potential. Int. J. Cancer 44, 707–713
17 Zeisig, R., Koklic, T., Wiesner, B., Fichtner, I. and Sentjurc, M. (2007) Increase in fluidity in the membrane of MT3 breast cancer cells correlates with enhanced cell adhesion *in vitro* and increased lung metastasis in NOD/SCID mice. Arch. Biochem. Biophys. 459, 98–106
18 Sade, A., Banerjee, S. and Severcan, F. (2010) Concentration-dependent differing actions of the nonsteroidal anti-inflammatory drug, celecoxib, in distearoyl phosphatidylcholine multilamellar vesicles. J. Liposome Res. 20, 168–177
19 Goormaghtigh, E., Raussens, V. and Ruysschaert, J. M. (1999) Attenuated total reflection infrared spectroscopy of proteins and lipids in biological membranes. Biochim. Biophys. Acta 1422, 105–185
20 Wood, B. R., Chiriboga, L., Yee, H., Quinn, M. A., McNaughton, D. and Diem, M. (2004) Fourier transform infrared (FTIR) spectral mapping of the cervical transformation zone, and dysplastic squamous epithelium. Gynecol. Oncol. 93, 59–68
21 Babrah, J., McCarthy, K., Lush, R. J., Rye, A. D., Bessant, C. and Stone, N. (2009) Fourier transform infrared spectroscopic studies of T-cell lymphoma, B-cell lymphoid and myeloid leukaemia cell lines. Analyst 134, 763–768
22 Ozek, N. S., Tuna, S., Erson-Bensan, A. E. and Severcan, F. (2010) Characterization of microRNA-125b expression in MCF7 breast cancer cells by ATR-FTIR spectroscopy. Analyst 135, 3094–3102
23 Gasper, R., Mijatovic, T., Benard, A., Derenne, A., Kiss, R. and Goormaghtigh, E. (2010) FTIR spectral signature of the effect of cardiotonic steroids with antitumoral properties on a prostate cancer cell line. Biochim. Biophys. Acta 1802, 1087–1094
24 Gao, T. Y., Feng, J. and Ci, Y. X. (1999) Human breast carcinomal tissues display distinctive FTIR spectra: implication for the histological characterization of carcinomas. Anal. Cell. Pathol. 18, 87–93
25 Argov, S., Ramesh, J., Salman, A., Sinelnikov, I., Goldstein, J., Guterman, H. and Mordechai, S. (2002) Diagnostic potential of Fourier-transform infrared microspectroscopy and advanced computational methods in colon cancer patients. J. Biomed. Opt. 7, 248–254
26 Severcan, F. and Cannistraro, S. (1990) A spin label ESR and saturation transfer ESR study of α-tocopherol containing model membranes. Chem. Phys. Lipids 53, 17–26
27 Gaigneaux, A., Ruysschaert, J. M. and Goormaghtigh, E. (2002) Infrared spectroscopy as a tool for discrimination between sensitive and multiresistant K562 cells. Eur. J. Biochem. 269, 1968–1973
28 Ogura, R., Sugiyama, M., Sakanashi, T. and Ninomiya, T. (1988) ESR spin-labeling method of determining membrane fluidity in biological materials: tissue culture cells, cardiac mitochondria, erythrocytes and epidermal cells. Kurume Med. J. 35, 171–182
29 Rossi, S., Giuntini, A., Balzi, M., Becciolini, A. and Martini, G. (1999) Nitroxides and malignant human tissues: electron spin resonance in colorectal neoplastic and healthy tissues. Biochim. Biophys. Acta 1472, 1–12
30 Severcan, F. and Cannistraro, S. (1988) Direct electron-spin resonance evidence for α-tocopherol-induced phase-separation in model membranes. Chem. Phys. Lipids. 47, 129–133
31 Cimen, I., Tuncay, S. and Banerjee, S. (2009) 15-Lipoxygenase-1 expression suppresses the invasive properties of colorectal carcinoma cell lines HCT-116 and HT-29. Cancer Sci. 100, 2283–2291
32 Lopezgarcia, F., Micol, V., Villalain, J. and Gomezfernandez, J. C. (1993) Infrared spectroscopic study of the interaction of diacylglycerol with phosphatidylserine in the presence of calcium. Biochim. Biophys. Acta 1169, 264–272
33 Severcan, F., Kazanci, N. and Zorlu, F. (2000) Tamoxifen increases membrane fluidity at high concentrations. Biosci. Rep. 20, 177–184
34 Zhao, L. Y., Feng, S. S., Kocherginsky, N. and Kostetski, I. (2007) DSC and EPR investigations on effects of cholesterol component on molecular interactions between paclitaxel and phospholipid within lipid bilayer membrane. Int. J. Pharm. 338, 258–266

35 Niederberger, E., Tegeder, I., Vetter, G., Schmidtko, A., Schmidt, H., Euchenhofer, C., Brautigam, L., Grosch, S. and Geisslinger, G. (2001) Celecoxib loses its anti-inflammatory efficacy at high doses through activation of NF-κB. FASEB J. 15, 1622
36 Steinbach, G., Lynch, P. M., Phillips, R. K. S., Wallace, M. H., Hawk, E., Gordon, G. B., Wakabayashi, N., Saunders, B., Shen, Y., Fujimura, T. et al. (2000) The effect of celecoxib, a cyclooxygenase-2 inhibitor, in familial adenomatous polyposis. N. Engl. J. Med. 342, 1946–1952
37 Maier, T. J., Schiffmann, S., Birod, K., Angioni, C., Hoffmann, M., Lopez, J. J., Glaubitz, C., Steinhilber, D., Geisslinger, G. and Grosch, S. (2009) Celecoxib accumulates in phospholipid membranes of human colorectal cancer cells. Naunyn-Schmiedebergs Arch. Pharmacol. 379, 486
38 Gazi, E., Baker, M., Dwyer, J., Lockyer, N. P., Gardner, P., Shanks, J. H., Reeve, R. S., Hart, C. A., Clarke, N. W. and Brown, M. D. (2006) A correlation of FTIR spectra derived from prostate cancer biopsies with Gleason grade and tumour stage. Eur. Urol. 50, 750–761
39 Garip, S. and Severcan, F. (2010) Determination of simvastatin-induced changes in bone composition and structure by Fourier transform infrared spectroscopy in rat animal model. J. Pharm. Biomed. Anal. 52, 580–588
40 Sok, M., Sentjurc, M., Schara, M., Stare, J. and Rott, T. (2002) Cell membrane fluidity and prognosis of lung cancer. Ann. Thorac. Surg. 73, 1567–1571
41 Wiseman, H., Quinn, P. and Halliwell, B. (1993) Tamoxifen and related-compounds decrease membrane fluidity in liposomes – mechanism for the antioxidant action of tamoxifen and relevance to its anticancer and cardioprotective actions. FEBS Lett. 330, 53–56
42 Kanwar, S. S., Vaiphei, K., Nehru, B. and Sanyal, S. N. (2007) Chemopreventive effects of nonsteroidal anti-inflammatory drugs in the membrane lipid composition and fluidity parameters of the 1,2-dimethylhydrazine-induced colon carcinogenesis in rats. Drug Chem. Toxicol. 30, 293–309
43 Sherbet, G. V. (1989) Membrane fluidity and cancer metastasis. Exp. Cell Biol. 57, 198–205
44 Chuang, H. C., Kardosh, A., Gaffney, K. J., Petasis, N. A. and Schonthal, A. H. (2008) COX-2 inhibition is neither necessary nor sufficient for celecoxib to suppress tumor cell proliferation and focus formation *in vitro*. Mol. Cancer. 7, 38
45 Dianzani, C., Brucato, L., Gallicchio, M., Rosa, A. C., Collino, M. and Fantozzi, R. (2008) Celecoxib modulates adhesion of HT29 colon cancer cells to vascular endothelial cells by inhibiting ICAM-1 and VCAM-1 expression. Br. J. Pharmacol. 153, 1153–1161
46 Anderson, R. G. W. and Jacobson, K. (2002) A role for lipid shells in targeting proteins to caveolae, rafts, and other lipid domains. Science 296, 1821–1825
47 Katsu, T., Imamura, T., Komagoe, K., Masuda, K. and Mizushima, T. (2007) Simultaneous measurements of K^+ and calcein release from liposomes and the determination of pore size formed in a membrane. Anal. Sci. 23, 517–522
48 Kulp, S. K., Yang, Y. T., Hung, C. C., Chen, K. F., Lai, J. P., Tseng, P. H., Fowble, J. W., Ward, P. J. and Chen, C. S. (2004) 3-Phosphoinositide-dependent protein kinase-1/Akt signaling represents a major cyclooxygenase-2-independent target for celecoxib in prostate cancer cells. Cancer Res. 64, 1444–1451
49 Kundu, N., Smyth, M. J., Samsel, L. and Fulton, A. M. (2002) Cyclooxygenase inhibitors block cell growth, increase ceramide and inhibit cell cycle. Breast Cancer Res. Treat. 76, 57–64
50 Kim, S. H., Song, S. H., Kim, S. G., Chun, K. S., Lim, S. Y., Na, H. K., Kim, J. W., Surh, Y. J., Bang, Y. J. and Song, Y. S. (2004) Celecoxib induces apoptosis in cervical cancer cells independent of cyclooxygenase using NF-κB as a possible target. J. Cancer Res. Clin. Oncol. 130, 551–560
51 Lee, A. G. (2004) How lipids affect the activities of integral membrane proteins. Biochim. Biophys. Acta 1666, 62–87

Received 14 December 2010/10 March 2011; accepted 15 March 2011
Published as Immediate Publication 15 March 2011, doi 10.1042/BSR20100149

 ©The Authors Journal compilation ©2012 Biochemical Society

Biosci. Rep. (2012) / **32** / 35–44 (Printed in Great Britain) / doi 10.1042/BSR20100149

online data

Original Paper

SUPPLEMENTARY ONLINE DATA

Celecoxib reduces fluidity and decreases metastatic potential of colon cancer cell lines irrespective of COX-2 expression

Aslı SADE, Seda TUNÇAY, İsmail ÇIMEN, Feride SEVERCAN and Sreeparna BANERJEE[1]

Department of Biological Sciences, Middle East Technical University, Ankara 06531, Turkey

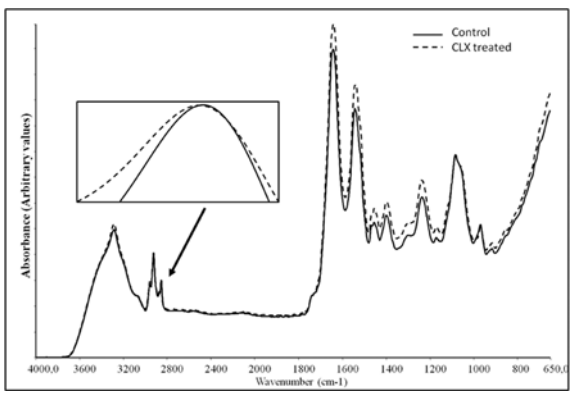

Figure S1 Representative FTIR spectra of control and 20 μM CLX-treated HT29 cells
The arrow shows the CH_2 symmetric stretching band that is expanded in the inset.

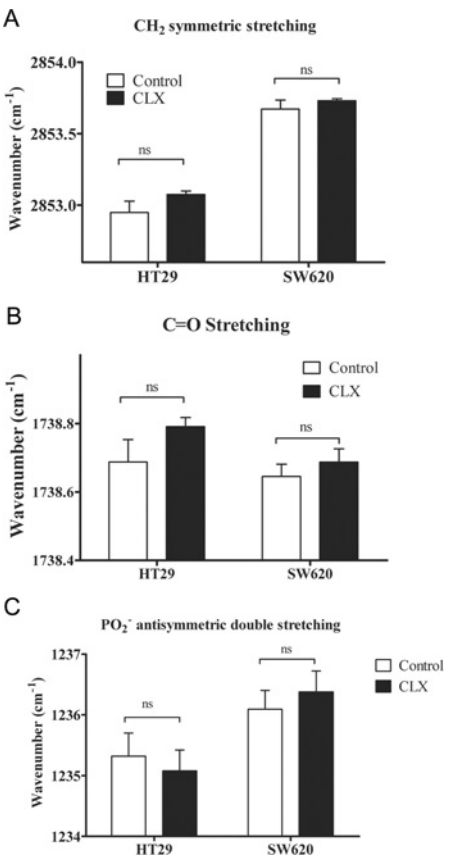

Figure S2 CLX treatment does not change the acyl chain flexibility (A) or the hydration status of the glycerol backbone (B) or lipid head groups (C)
The average frequency changes in (A) CH_2 symmetric stretching, (B) C = O stretching and (C) PO_2^- antisymmetric double-stretching mode resulting from a 24 h treatment of HT29 and SW620 cells with 20 μM CLX; each point represents the mean$\pm$S.E.M. (n = 5). ns, not significant.

[1] To whom correspondence should be addressed (email banerjee@metu.edu.tr).

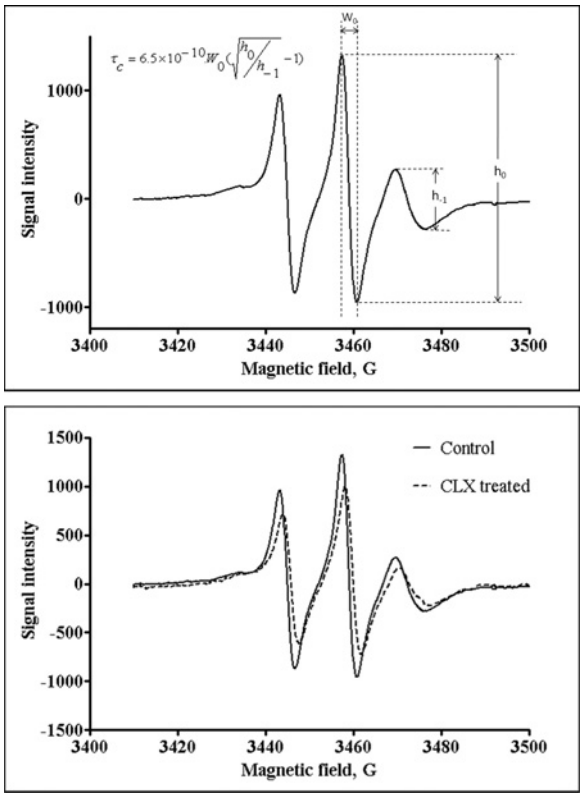

Figure S3 Representative SL-ESR spectra of control and CLX-treated HT29 cells

(A) Representative ESR spectrum from a control cell line (HT29) showing the equation used to determine the rotational correlation time. (B) Representative ESR spectra showing the changes in the spectral parameters upon treatment with CLX.

Received 14 December 2010/10 March 2011; accepted 15 March 2011
Published as Immediate Publication 15 March 2011, doi 10.1042/BSR20100149

©The Authors Journal compilation ©2012 Biochemical Society